Nano-lubricant film formation due to combined elastohydrodynamic and surface force action under isothermal conditions

M F Abd-AlSamieh and **H Rahnejat***
Wolfson School of Mechanical and Manufacturing Engineering, Loughborough University, Loughborough, UK

Abstract: This paper presents the results of numerical prediction of the lubricant film thickness and pressure distribution in concentrated counterformal point contact under isothermal conditions. The operating conditions, which include load and speed of entraining motion, promote the formation of ultra-thin films; these are formed under the combined action of elastohydrodynamic lubrication (EHL), the surface contact force of solvation and molecular interactions due to the presence of Van der Waals forces. A numerical solution has been carried out, using the low-relaxation Newton–Raphson iteration technique, applied to the convergence of the hydrodynamic pressure. The paper shows that the effect of surface forces become significant as the elastic film (i.e. the gap) is reduced to a few nanometres. The numerical predictions have been shown to conform well to the numerical work and experimental findings of other research workers.

Keywords: ultra-thin films, elastohydrodynamics, solvation, Van der Waals force

NOTATION

a	lubricant molecular diameter
A	Hamaker constant
b	radius of Hertzian contact region
C	constant defined in equation (11)
D	deformation influence coefficient matrix
$E_{A,B}$	Young's modulus of elasticity of contiguous bodies
E'	reduced modulus of elasticity $= \dfrac{2}{(1-\nu_A^2)/E_A + (1-\nu_B^2)/E_B}$
G^*	materials' parameter $= E'\alpha$
h	lubricant film thickness
H	dimensionless film thickness $= hR/b^2$
H_0	dimensionless central oil-film thickness
l	dimensionless side leakage boundary distance
m	dimensionless inlet distance
n_x, n_y	number of computational grid nodes
N	total number of mesh points
p	total contact pressure
p_h	hydrodynamic pressure
p_s	solvation pressure due to the interaction force of the surfaces
p_{vdw}	pressure due to molecular Van der Waals force
P	dimensionless total contact pressure $= p/P_{Her}$
P_h	dimensionless hydrodynamic pressure $= p_h/P_{Her}$
P_{Her}	maximum Hertzian contact pressure
P_s	dimensionless solvation pressure $= p_s/P_{Her}$
P_{vdw}	dimensionless Van der Waals pressure $= p_{vdw}/P_{Her}$
R	reduced radius of counterformal contact
u	speed of entraining motion $= \frac{1}{2}(u_A + u_B)$
U^*	speed (or rolling viscosity) parameter $= u\eta_0/(E'R^2)$
w	normal applied contact load
W^*	load parameter $= w/(E'R^2)$
X, Y	dimensionless coordinates, $X = x/b$, $Y = y/b$
Z	viscosity–pressure index
α	lubricant piezo-viscosity index
δ	total elastic deformation
ε, ξ	constants used in equation (3)
η	lubricant dynamic viscosity
η_0	atmospheric lubricant dynamic viscosity

The MS was received on 14 December 2000 and was accepted after revision for publication on 7 March 2001.
**Corresponding author: Wolfson School of Mechanical and Manufacturing Engineering, Loughborough University, Loughborough, Leicestershire LE11 3TU, UK.*

ν	Poisson's ratio
$\bar{\eta}$	dimensionless lubricant viscosity $= \eta/\eta_0$
ρ	lubricant density
ρ_0	atmospheric lubricant density
$\bar{\rho}$	dimensionless lubricant density $= \rho/\rho_0$
Ω	under-relaxation factor

Superscripts

i, j	contravariant influence coefficient indices
n	iteration index

Subscripts

A, B	denote the contiguous bodies in contact
k, l	covariant influence coefficient indices

1 INTRODUCTION

In recent years there has been a growing trend toward component miniaturization in the manufacture of increasingly compact and lightweight machines. This has opened new fields of engineering endeavour such as microengineering and nanotechnology, with diverse applications. As a consequence, the operational separation of load surfaces has reduced considerably. Lubricated contact characteristics were previously dominated by the elastohydrodynamic mechanism of lubrication, with oil films tenths of a micrometre thick; separations have now decreased to a few to tens of nanometres. Under these conditions, lubricant behaviour is no longer governed purely by its bulk properties, such as density and viscosity. The effect of surface forces in vanishingly small gaps and the action of molecular forces have become significant. Under these conditions, lubricant film formation is governed by a new multiphysics phenomenon, which includes the physical properties of the solid surfaces and the molecular chemistry of the lubricant, as well as its layering properties.

Typical examples of mechanisms in which nanotribology plays an important role include high-performance gears, hard disk drive systems in magnetic storage media, in which the flying height of a magnetic head over a disk surface approaches a few or a few tens of nanometres, and in particular a system in which the hard disk interface may be immersed in liquid lubricant instead of air. The separation between the surfaces in such cases is on the nanometre scale—of the order of the molecular diameter of the intervening liquid.

Studies carried out by Chan and Horn [**1**] have shown that, for molecularly smooth surfaces, the Reynolds equation seems to apply down to a film thickness of 50 nm, and with simple correction factors can be applied even further down to several nanometres. At closer distances, the attractive Van der Waals force and the oscillatory (attraction–repulsion) solvation force become the dominant mechanisms in lubricant film formation. Jang and Tichy [**2**] have presented a full numerical solution for the problem of elastohydrodynamic lubrication (EHL), including the effect of the Van der Waals force and solvation pressure. However, their investigation shows little influence of surface and molecular forces, even down to a film thickness of 2 nm. This finding is not in accord with the conclusions in reference [**1**] and work reported by other workers, such as Matsuoka and Kato [**3**]. This difference is probably due to the fact that Jang and Tichy [**2**] used a lubricant with a relatively high value of bulk viscosity.

Matsuoka and Kato [**3**] have developed a new method for calculating the total pressure as a combined effect of EHL and the solvation surface force. They found that when the film thickness is greater than 10 nm, there is good agreement with the conventional continuum fluid lubrication theory (EHD theory), but with film thickness less than 10 nm, deviation occurs between their theoretical predictions based upon EHL alone and the experimental evidence. However, when they included the effect of solvation pressure, better agreement was obtained with the experimental results.

Experimental studies reported by Dalmaz [**4**], measuring film thickness values down to 50 nm, agree well with theoretical predictions when Hamrock and Dowson's [**5**] extrapolated oil-film thickness expression is employed. Johnston *et al.* [**6**] have shown that down to 15 nm the measured film thickness conforms to the same theoretical predictions, and that below this value there is apparently an even stronger dependence on the speed of the entraining motion. They have suggested that the continuum assumption in the theory of hydrodynamics loses its validity under these conditions and the lubricant layering results in changes in its viscosity, different from its bulk value. Further experimental investigations by Cooper and Moore [**7**] indicate that down to 10 nm the lubricant film thickness agrees well with theoretical predictions. A number of researchers [**8**, **9**] have shown that, with certain lubricants, the effect of surface forces is negligible, and that the lubricant film behaviour follows the EHL theory down to a thickness of 1 nm. A physical explanation for this has been put forward by Christenson *et al.* [**10**] and Gee *et al.* [**11**]. They suggest that these lubricants, which have either a chain or a branched structure, become entangled owing to their flexibility, and so exhibit little solvation effect adjacent to the solid surface.

Recently, Kato and Matsouka [**12**–**14**] have developed a new apparatus for the measurement of inter-surface forces and film thickness. They have found that when the measured lubricant film thickness is larger than 10 nm, it is in accord with the EHL theory. Discretization of the film was observed when its thickness was reduced to only a few nanometres. These findings corroborated the theoretical predictions in reference [**3**].

The aforementioned numerical solutions [**2**, **3**] both employ the Voghepol transformation $\phi = PH^{3/2}$ in the solution of Reynolds' hydrodynamic equation. The method of solution employed in both cases is by Gaussian elimination, which has been found to be suitable at low external loads and moderate-to-high speeds of entraining motion. At higher values of load and particularly low speeds of entraining motion, this method has been found to be computationally unstable with convergence problems. For thin films with rolling speeds at 0.2–8 mm/s, such as those reported in this paper, it is more appropriate to use a low-relaxation Newton–Raphson method with Gauss–Seidel iterations to solve for the EHL contribution. In this paper a large range of loads (0.01–20 N) and speeds (0.2–8 mm/s) are employed to investigate the onset of lubricant discretization. The solution method includes the effect of solvation pressure, as well as the Van der Waals force.

2 THEORETICAL BASIS

In conventional EHL theory, film thickness and pressure distribution are obtained by simultaneous solution of the Reynolds equation; the elastic film shape, incorporating the contact deformation of the semi-infinite solid (given by the elasticity equation); and the load balance equation. However, in the case of ultra-thin film thickness, a pressure caused by the Van der Waals intermolecular forces and a solvation pressure due to inter-surface forces should also be considered. The total pressure, P, is composed of three components: solvation pressure P_s, Van der Waals pressure contribution P_{vdw} and conventional viscous pressure P_h:

$$P = P_s + P_{vdw} + P_h \tag{1}$$

The use of the above equation is justified by the fact that the load carried by the lubricant is supported by all the mechanisms that contribute to the formation of the lubricant film through generation of pressure. In the case of the Van der Waals force, the attractive nature of the force leads to suction (i.e. negative pressures). The oscillatory nature of solvation can also contribute to such an effect. Negative pressures reduce the load-carrying capacity. The repulsive net total pressure contribution therefore balances the constant applied load under steady state entraining, according to Newton's third axiom. This yields the gap size. Therefore, use of equation (1) is justified by Bernoulli's principle of superposition.

The use of EHL theory is also justified in this analysis, as Newtonian continuum mechanics holds true for viscous flow of fluids in any conjunction where the physics of motion is described by the relative motion of hard, spherical molecules and with a thickness in excess of two molecular diameters of the intervening fluid. In such narrow gaps the effects of the Van der Waals force and the electrostatic double-layer forces begin to dominate. As the film thickness is reduced further, the ensuing unstructured environment contravenes both the Newtonian viscous flow model and the Lifshitz structureless continuum theory. In such cases, the use of EHL theory becomes suspect. This paper, therefore, presents analyses that remain within the fold of Newtonian fluid flow in a continuum. As the combined surface roughness of the mating mica surfaces remain insignificant (less than a third of the lubricant film thickness, see the results section, and note that the surface roughness is in the region 0.048–0.6 nm), the need for a micro-EHL analysis does not arise. This point is considered in more detail in the results section.

2.1 Elastohydrodynamic pressure

The dimensionless Reynolds equation for point contact condition under steady state entraining can be written as

$$\frac{\partial}{\partial X}\left(\frac{\bar{\rho}H^3}{\bar{\eta}}\frac{\partial P_h}{\partial X}\right) + \frac{\partial}{\partial Y}\left(\frac{\bar{\rho}H^3}{\bar{\eta}}\frac{\partial P_h}{\partial Y}\right) = \lambda\frac{\partial}{\partial X}(\bar{\rho}H) \tag{2}$$

where the following dimensionless variables apply:

$$X = x/b, \qquad Y = y/b, \qquad \bar{\eta} = \frac{\eta}{\eta_0}$$

$$\bar{\rho} = \frac{\rho}{\rho_0}, \qquad H = hR/b^2, \qquad P_h = p_h/p_{Her}$$

and

$$\lambda = \frac{12u\eta_0 R^2}{b^3 P_{Her}}$$

The variation in density of the lubricant with pressure is defined by Dowson and Higginson [**15**] as

$$\bar{\rho} = 1 + \frac{\varepsilon P_h P_{Her}}{1 + \xi P_h P_{Her}} \tag{3}$$

where ε and ζ are constants, dependent upon the type of lubricant used. The variation in the viscosity of the lubricant with pressure in dimensionless form is given by Roelands [**16**] as

$$\bar{\eta} = \exp(\ln\eta_0 + 9.67)\lfloor(1 + 5.1\times10^{-9}P_h P_{Her})^Z - 1\rfloor \tag{4}$$

where

$$Z = \frac{\alpha}{5.1\times10^{-9}(\ln\eta_0 + 9.67)}$$

The elastic film shape in dimensionless form is assumed to be the same as that reported by Hamrock and

Dowson [5], given by

$$H(X, Y) = H_0 + \frac{(X-m)^2}{2} + \frac{(Y-l)^2}{2} + \frac{R\delta(X, Y)}{b^2} \quad (5)$$

where the dimensional elastic deformation at any point x, y is defined by Hamrock and Dowson [5] as

$$\delta_{I,J}(x, y) = \frac{2}{\pi} P_{\text{Her}} \sum_{j=1,2}^{ny} \sum_{i=1,2}^{nx} P_{i,j} D_{i^*,j^*} \quad (6)$$

where

$$i^* = |I - i| + 1, \qquad j^* = |J - j| + 1$$

The Newton–Raphson method is applied to the solution of the Reynolds' equation in the following numerical form:

$$\sum_{l=2}^{my-1} \sum_{k=2}^{mx-1} J_{k,l}^{i,j} \Delta P_{k,l} = -F_{i,j} \quad (7)$$

where the Jacobian matrix is a tensorial quantity, given in terms of the residual derivatives as

$$J_{k,l}^{i,j} = \frac{\partial F_{i,j}}{\partial P_{\text{h}_{k,l}}} \quad (8)$$

Using the Gauss–Seidel iteration method, the system state equation can be written as

$$\Delta P_{k,l}^{n} = \frac{\begin{array}{c} -F_{i,j} - J_{k-1,l}^{i,j} \Delta P_{k-1,l}^{n} - J_{k+1,l}^{i,j} \Delta P_{k+1,l}^{n-1} \\ - J_{k,l-1}^{i,j} \Delta P_{k,l-1}^{n} - J_{k,l+1}^{i,j} \Delta P_{k,l+1}^{n-1} \end{array}}{J_{k,l}^{i,j}} \quad (9)$$

where n is the iteration counter in the above recursive equation.

To achieve good numerical stability, an under-relaxation factor is employed to update the pressure according to

$$P_{\text{h}_{i,j}}^{n} = P_{\text{h}_{i,j}}^{n-1} + \Omega \Delta P_{i,j}^{n} \quad (10)$$

where Ω is the under-relaxation factor, typically chosen as 0.01 under the conditions reported in this paper.

The convergence criterion on the pressure is

$$\left[\frac{\sum_i \sum_j (P_{\text{h}_{i,j}}^{n} - P_{\text{h}_{i,j}}^{n-1})^2}{N} \right]^{0.5} \leqslant 10^{-4}$$

The convergence criterion on load balance is given by

$$\left| \int \int P(X, Y) \, \text{d}X \, \text{d}Y - \frac{2}{3}\pi \right| \leqslant 10^{-4}$$

2.2 Solvation pressure

Solvation force (i.e. structural force) is a surface interaction force that acts between two solid surfaces when they approach each other to form a very small gap filled by a fluid. Horn and Israelachvili [17], Christenson *et al.* [10], Van Megen and Snook [18], Israelachvili *et al.* [19], Israelachvili [20] and Homola *et al.* [21] have studied the solvation force in the narrow conjunction of contiguous bodies. They have all shown that these surface forces generally have a decaying oscillatory characteristic as a function of gap (i.e. the film thickness). They vary as attractive and repulsive forces, with a periodicity equal to the mean diameter of the fluid molecules. Such oscillatory forces arise from the molecular geometry and local structure of the liquid medium, and reflect the forced ordering of the liquid molecules into discrete layers when constrained between two surfaces.

The solvation pressure is obtained as

$$P_{\text{s}} = -C \text{e}^{-h/a} \cos\left(\frac{2\pi h}{a}\right) \quad (11)$$

where for octamethylcyclotetrasiloxane (OMCTS), $a = 1$ nm and $C = 172$ MPa [1, 2, 17].

2.3 Van der Waals pressure

Van der Waals forces of attraction exist between two surfaces when they are separated by a very thin fluid film (see, for example, Lifshitz [22]). Israelachvili [20] gives an expression for the pressure in the fluid, induced by the Van der Waals forces, as a function of separation:

$$P_{\text{vdw}} = \frac{-A}{6\pi h^3} \quad (12)$$

For OMCTS, $A = 10^{-20}$ J [1, 17].

The total pressure in equation (1) is calculated simultaneously with the elastic film shape equation (5). This is the same procedure as that carried out for the conventional solution to the EHL problem.

3 RESULTS AND DISCUSSION

Figure 1 shows the total pressure distribution and the corresponding lubricant film thickness in the direction of entraining motion through the central film, obtained for the model parameters $a = 1$ nm, $C = 172$ MPa, and for the governing conditions $W^* = 0.2949 \times 10^{-7}$ and $U^* = 0.1871 \times 10^{-11}$. Those depicted by Fig. 1a are

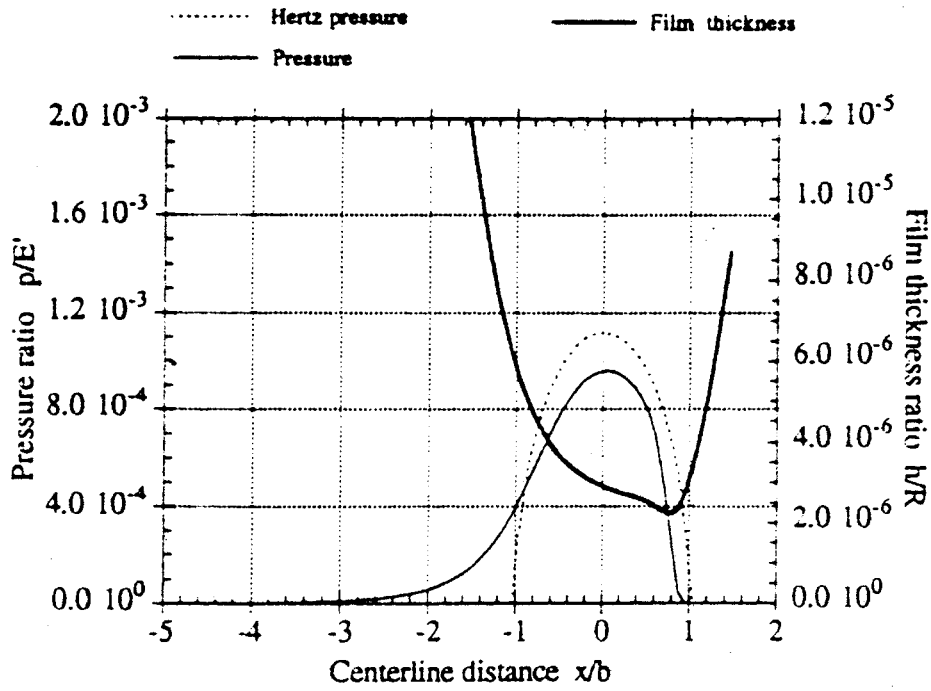

a) Jang and Tichy (2)

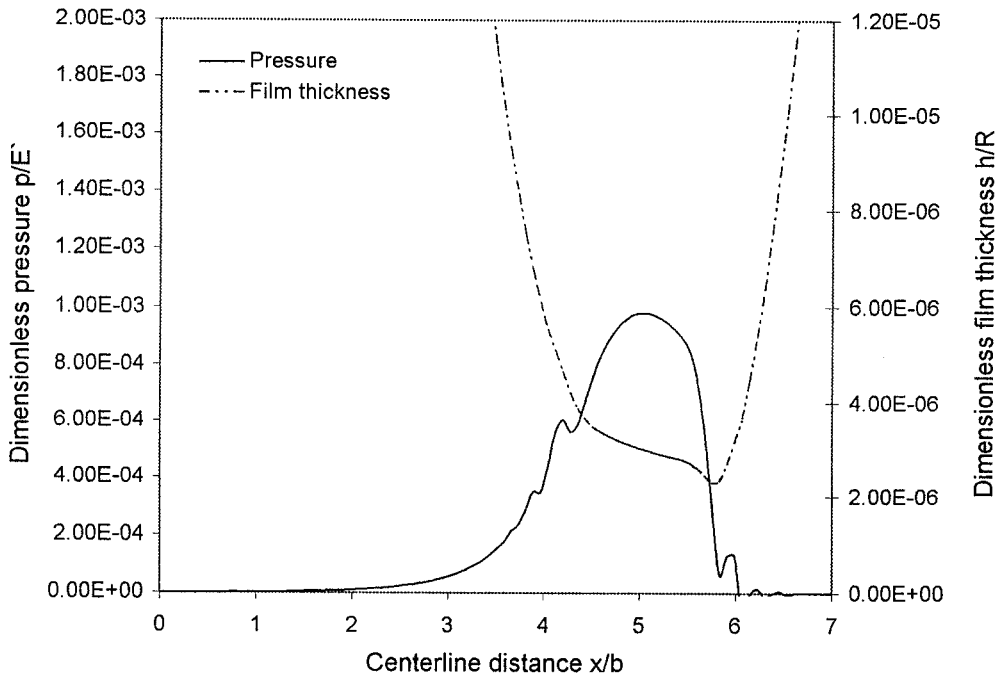

b) Current analysis

Fig. 1 Pressure profile and film thickness for $W^* = 0.2949 \times 10^{-7}$ and $U^* = 0.1871 \times 10^{-11}$

Table 1 Lubricant properties

Property	Value
Viscosity, η_o	0.0411 Pa s
Pressure of viscosity coefficient, α	0.11 GPa^{-1}
ε	5.83×10^{-10} Pa
ξ	1.68×10^{-9} Pa
Molecular diameter, a	1 nm

Table 2 Material properties

Property	Value
Young's modulus, E_A	0.20×10^{12} Pa
Young's modulus, E_B	0.20×10^{12} Pa
Poisson's ratio, ν_A	0.3
Poisson's ratio, ν_B	0.3
Radius of ball, R	0.005 m

the results obtained by Jang and Tichy [**2**], while those illustrated in Fig. 1b are obtained in the current analysis. Lubricant and material properties are given in Tables 1 and 2. As can be observed, very good agreement exists between both sets of results. In fact the minimum film thickness is obtained as 1.142 nm in the current analysis, and as 1.1 nm in reference [**2**]. It can be observed that, under these conditions, the elastohydrodynamic contribution dominates the generation of contact pressure. Jang and Tichy [**2**] have ignored the effect due to the viscosity of the mineral oil used by them; the value was 0.0411 Pa s. The analysis in Fig. 1b has imposed their iso-viscous conditions for the purpose of comparison, by letting $\alpha \approx 1.1 \times 10^{-12}$ m^2/N, thus giving $G^* = 0.242$. However, the effect of viscosity variation with respect to pressure should not have been ignored. When this was included in the current analysis, pertaining to full EHL conditions, the maximum pressure was increased by nearly 15 per cent, resulting in an increase in the minimum oil-film thickness of 0.6 nm (or 34 per cent). Figure 2 shows the central oil-film lubricant film thickness profile both with and without the effect of lubricant viscosity variation with pressure. The contribution due to solvation pressure is about 5 per cent, with insignificant change in film thickness. This is in line with findings of other research workers, that for higher-viscosity fluids the effect of surface forces is negligible and lubricant discretization does not take place [**3**, **8**, **9**].

In fact, Jang and Tichy [**2**] should not have employed the aforementioned model parameters for their mineral oil, since these parameters correspond to non-polar lubricants such as OMCTS. In order to obtain a more realistic comparison for the current analysis, it is necessary to use the correct viscosity of 2.35 mPa s for OMCTS and compare with the numerical predictions and experimental findings in references [**3**] and [**12**] to [**14**].

Figure 3 shows a comparison between the numerical predictions in reference [**3**] (Fig. 3a) and the current analysis (Fig. 3b) for total pressure distribution and the corresponding elastic film shape for the central line of contact. The model parameters are identical to the aforementioned values for a and C. The governing parameters are: $W^* = 2.77 \times 10^{-11}$ (i.e. 0.1 mN), $U^* = 1.305 \times 10^{-15}$ and $G^* = 360$ (for mica surfaces

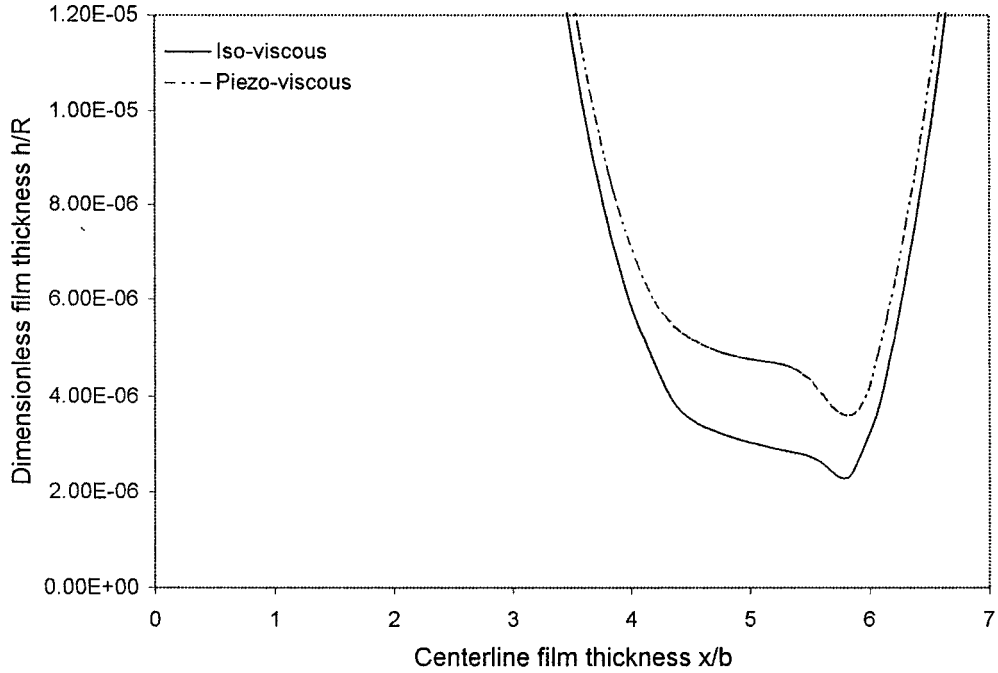

Fig. 2 Comparison between piezo-viscous and iso-viscous lubricants

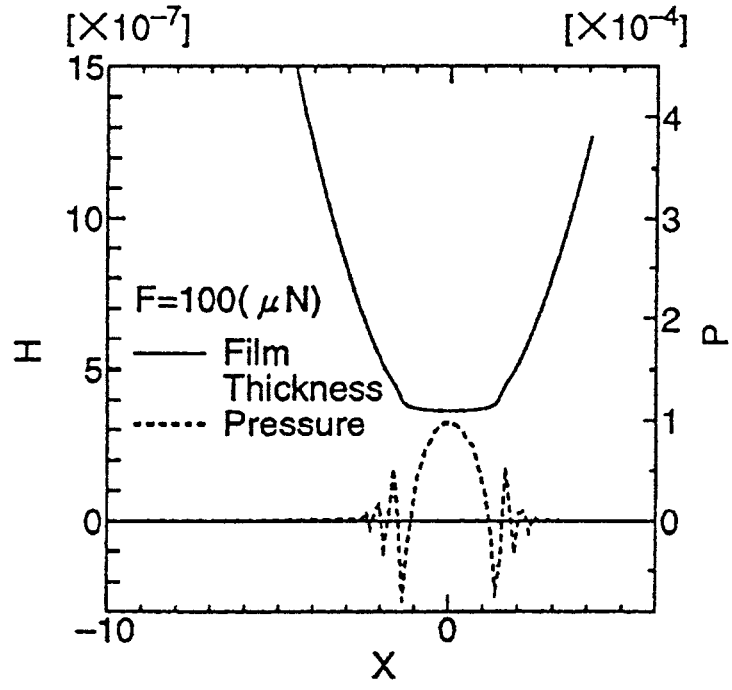

a) Matsuoka and Kato (3)

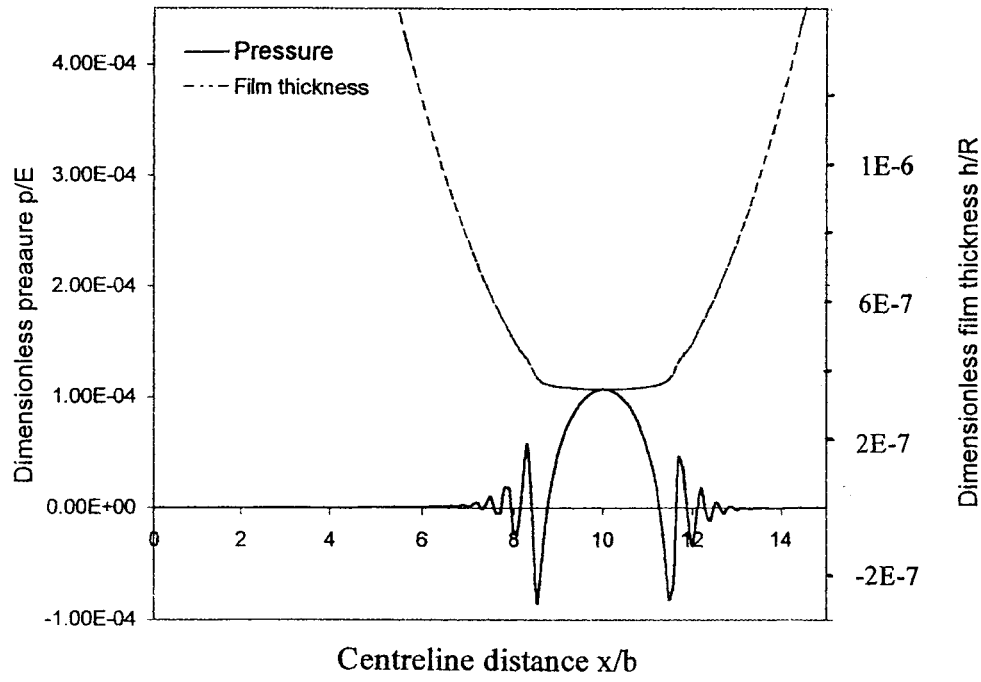

b) Current analysis

Fig. 3 Pressure profile and film thickness for $W^* = 2.77 \times 10^{-11}$ and $U^* = 1.305 \times 10^{-15}$

Table 3 Lubricant properties

Property	Value
Viscosity, η_o	2.35 mPa s
Pressure of viscosity coefficient, α	10 GPa^{-1}
ε	5.83×10^{-10} Pa
ξ	1.68×10^{-9} Pa
Molecular diameter, a	1 nm

Table 4 Material properties

Property	Value
Young's modulus, E_A	34.5 GPa
Young's modulus, E_B	34.5 GPa
Poisson's ratio, ν_A	0.205
Poisson's ratio, ν_B	0.205
Radius of ball, R	0.01 m

and $\alpha = 10$/GPa for OMCTS). Lubricant and material properties are provided in Tables 3 and 4. Very good agreement is obtained between both sets of analyses. In particular, they both exhibit the dominant role of solvation pressure under these conditions. The minimum lubricant film thickness is 3.6 nm, and the maximum total pressure is approximately 3.86 MPa. The contribution due to hydrodynamic pressure is very small, amounting to 0.25 MPa. For the same load, but with an increased speed of entraining motion, $U^* = 9.79 \times 10^{-15}$, the effect of EHL pressure becomes significant, resulting in a lubricant film thickness of 4.6 nm (more than 95 per cent of which is contributed by hydrodynamic pressure). Figure 4 shows the pressure distribution and film thickness for this condition.

A clearer picture emerges if, for a given value of load, the entraining speed is increased to obtain the demarcation boundary between the region dominated by EHL and that by the surface force action in the formation of lubricant film. Figure 5 shows such a plot of H against U^* for the value of $W^* = 2.77 \times 10^{-11}$ (i.e. 0.1 mN). It should be noted that the layering effect (i.e. discretization of the lubricant film) takes place at the lower values of entraining speed, up to $U^* \approx 10^{-14}$. This corresponds to a film thickness of approximately up to 4.6 nm. Thereafter, the viscous hydrodynamic effect gains in ascendancy and the film thickness varies linearly with increasing value of $U^* > 10^{-14}$. The characteristics here are completely governed by the hydrodynamic behaviour of the film.

Finally, the numerical predictions carried out here can be compared with the experimental and theoretical results in reference [**3**], which also incorporates results from the model employed by Jang and Tichy [**2**], and with those of Chan and Horn [**1**] (see Fig. 6, with lubricant OMCTS and mica contacting surfaces). In all cases the variation of the minimum oil-film thickness is shown for increasing values of applied load. It can be observed that as the applied load is increased at constant speed of entraining motion (200 μm/s), the film thickness is reduced and lubricant discretization appears. The effect of solvation becomes more dominant for film thickness around 4.6 nm in the current analysis, and around 7–8 nm in references [**2**] and [**3**]. At loads greater than 0.4 mN, the predicted film thickness is lower for the results reported in reference [**3**] than for the other analyses. Matsuoka and Kato [**3**] have attributed this difference to the effect of elastic deformation upon the solvation pressure, noting that the surface forces are overestimated when the effect of surface deformation

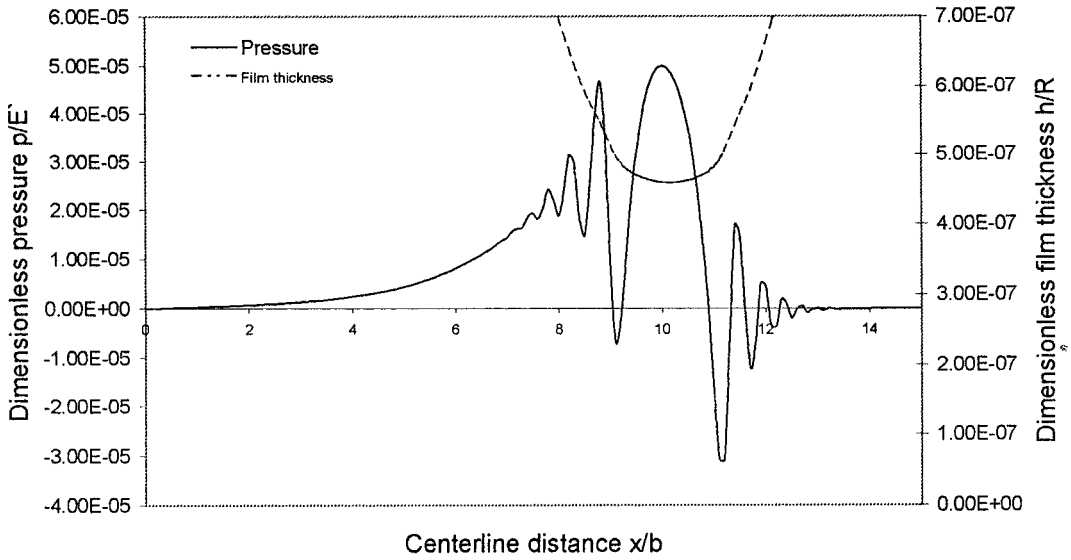

Fig. 4 Pressure profile and film thickness for $W^* = 2.77 \times 10^{-11}$ and $U^* = 9.79 \times 10^{-15}$

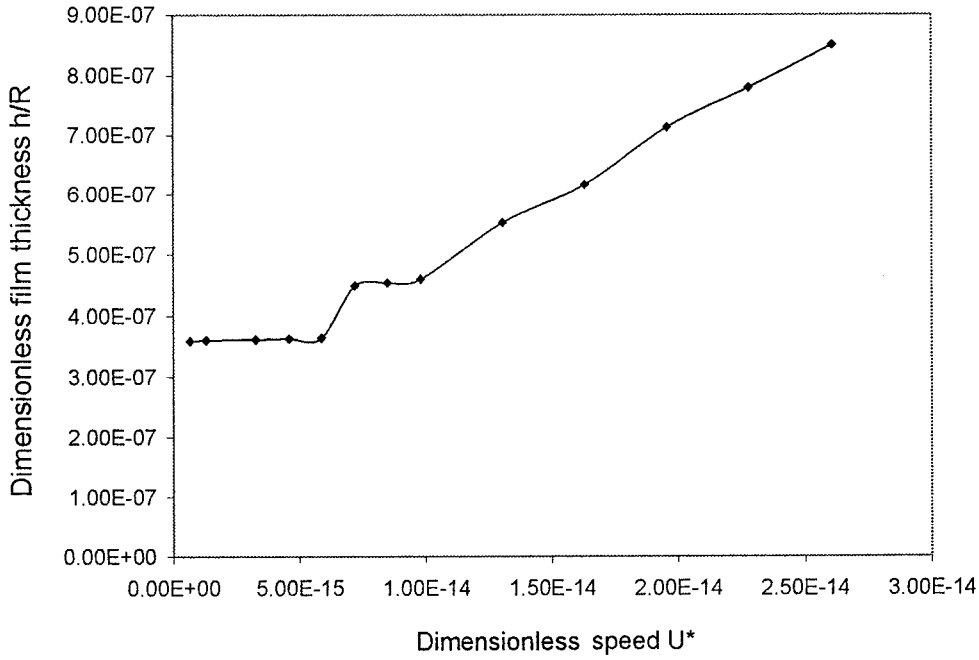

Fig. 5 Variation in film thickness with speed

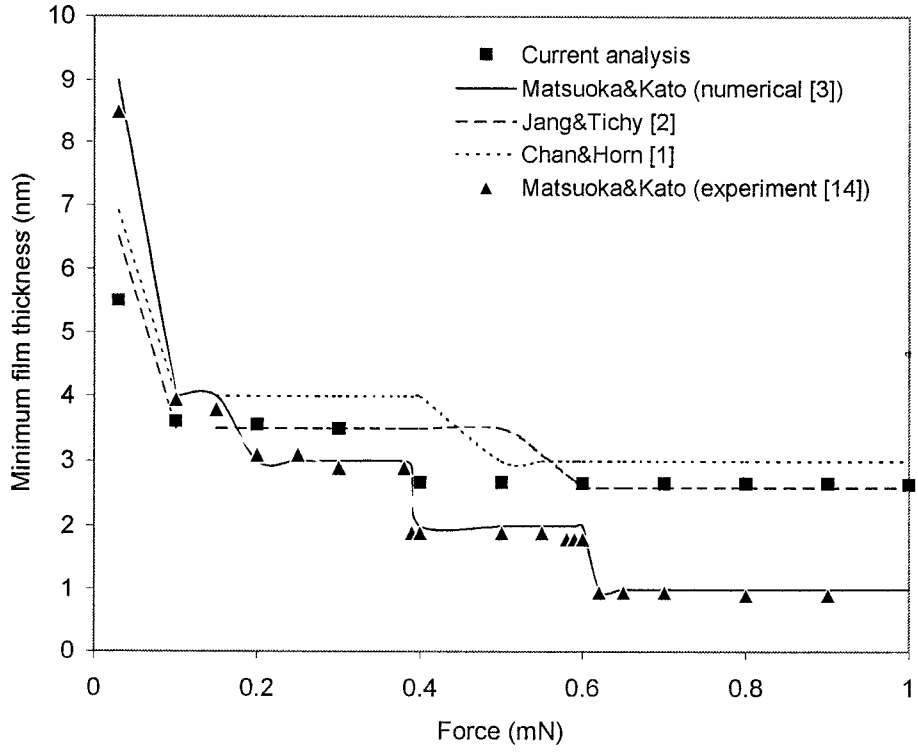

Fig. 6 Comparison between the current analysis and numerical/experimental results of other researchers

upon them is ignored. This would yield a larger total pressure in all the cases other than those obtained in reference [**3**], which, therefore, exhibits thinner films. This explanation is corroborated by the present analysis, which employs the same exponential–cosine solvation variation as in Chan and Horn [**1**] and Jang and Tichy [**2**]. In contrast, Matsuoka and Kato [**3**] have limited the domain of their calculation for elastic deformation to a region local to the point of calculation, in order to reduce the computational burden. This approach is necessary when the solution to the Reynolds' hydrodynamic equation is also based upon the Voghepol transformation, which is computationally time intensive. Determination of local deformation by the reduced

influence coefficient method, proposed initially by St Venant, is permissible for the results in Fig. 6 for loads greater than 0.4 mN, which fall into the iso-viscous elastic region, but they can only be regarded as approximate. The current analysis employs a full-domain solution and uses the Newton–Raphson method, which results in greater stability at higher load intensity. Thus, the elastic film shape obtained would be more accurate. More significantly, Matsuoka and Kato [**3**] retain their viscous contribution in arriving at a lubricant film thickness less than two molecular diameters of the intervening fluid at the higher values of load in Fig. 6. The observations in Section 2 show that their assumption of a continuum in such cases is not justified, as it abrogates the rigidity of the Newtonian hard molecular spheres. In this vanishing region of space–time the forces of solvation and electrostatic repulsion through ionization govern the molecular action by Brownian physics of motion. Their results could only be relied upon if such an approach were undertaken. However, the analysis presented in this paper does not need to be extended to such considerations, because the predicted films remain firmly within the bounds of both the Newtonian viscous flow model and the Lifshitz structureless continuum.

It should be noted that the use of mica surfaces ensures molecularly smooth surfaces. If this were not to be the case, the geometry on an asperity could become comparable in dimension to that of the radius of the Hertzian contact. The constancy of the speed of entraining motion would lose its physical meaning and the use of Reynolds' equation would become inappropriate. A more insurmountable problem would be that for a single asperity contact, the principal radii of curvature would become smaller than the dimensions of the Hertzian contact under the loads employed here. This fact, together with the low generated pressures observed, would lead to the breakdown of the validity of continuum mechanics. However, it is hoped that the results obtained in this paper show this not to be the case under the simulated conditions.

4 SUMMARY

In conclusion, it has been shown that the behaviour of lubricants, such as mineral oils, in concentrated counterformal contacts under load in the range 0.1–3 mN is governed by hydrodynamic effects. The effects of surface forces and molecular interaction are negligible. This finding conforms to the conclusions of Jang and Tichy [**2**]. This result is due to the high viscosity of such lubricants. However, with non-polar lubricants such as OMCTS, the lubricant behaviour goes through a transition, such that for the conditions investigated here, with separation decreasing from a value of 5 nm the effect of surface forces become dominant. The contribution due to the Van der Waals force remains small, even for lubricant films down to 3 nm thickness.

ACKNOWLEDGEMENTS

The authors would like to express their gratitude to the Egyptian Military Attaché's Office for the financial support extended to this research project.

REFERENCES

1 **Chan, D. Y. C.** and **Horn, R. G.** The drainage of thin liquid films between solid surfaces. *J. Chem. Phys.*, 1984, **83**, 5311–5324.
2 **Jang, S.** and **Tichy, J.** Rheological models for thin film EHL contacts. *Trans. ASME, J. Tribology*, 1995, **117**, 22–28.
3 **Matsuoka, H.** and **Kato, T.** An ultrathin liquid film lubrication theory—calculation method of solvation pressure and its application to the EHL problem. *Trans. ASME, J. Tribology*, 1997, **119**(1), 217–226.
4 **Dalmaz, G.** Film thickness and traction measurements in small elastohydrodynamic elliptical contacts. In Proceedings of the 5th Leeds–Lyon Symposium on *Tribology*, 1987, pp. 71–80.
5 **Hamrock, B. J.** and **Dowson, D.** Isothermal elastohydrodynamic lubrication of point contact. Part I—theoretical formulation. *Trans. ASME, J. Tribology*, 1976, **98**, 223–229.
6 **Johnston, G. J., Wayte, R.** and **Spikes, H. A.** The measurement and study of very thin lubricants films in concentrated contacts. *STLE Tribology Trans.*, 1991, **34**, 187–194.
7 **Cooper, D.** and **Moore, A. J.** Application of the ultrathin elastohydrodynamic oil film thickness technique to the study of automotive engine oils. *Wear*, 1994, **175**, 93–105.
8 **Guanteng, G.** and **Spikes, H. A.** Behaviour of lubricants in the mixed elastohydrodynamic regime. In Proceedings of 21st Leeds–Lyon Symposium on *Tribology*, Leeds, September 1994, pp. 479–485.
9 **Smeeth, M.** and **Spikes, H. A.** The formation of viscous surface films by polymer solutions: boundary or elastohydrodynamic lubrication. In STLE Annual Meeting, Chicago, 1995, paper 95-NP-7D-2.
10 **Christenson, H. K., Horn, R. G.** and **Israelachvili, J. N.** Measurement of forces due to structure in hydrocarbon liquids. *J. Colloid and Interface Sci.*, 1982, **88**, 79–88.
11 **Gee, M. L., Mcguiggan, P. M., Israelachvili, J. N.** and **Homola, A. M.** Liquid to solid like transition of molecularly thin films under shear. *J. Chem. Phys.*, 1990, **93**, 1895–1906.
12 **Matsuoka, H.** and **Kato, T.** Discrete nature of ultrathin lubrication film between mica surfaces. *Trans. ASME, J. Tribology*, 1996, **118**(4), 832–838.
13 **Matsuoka, H.** and **Kato, T.** Experimental study of ultrathin liquid lubrication film thickness at the molecular scale. *Proc. Instn Mech. Engrs, Part J, Journal of Engineering Tribology*, 1997, **211**(J2), 139–150.
14 **Kato, T.** and **Matsuoka, H.** Molecular layering in thin-film elastohydrodynamics. *Proc. Instn Mech. Engrs, Part J, Journal of Engineering Tribology*, 1999, **213**(J6), 363–370.

15 **Dowson, D.** and **Higginson, G. R.** A numerical solution to the elastohydrodynamic problem. *J. Mech. Engng Sci.*, 1959, **1**, 6–15.
16 **Roelands, C. J. A.** Correlation aspects of viscosity-temperature-pressure relationship of lubricating oils. PhD thesis, Delft University of Technology, The Netherlands, 1966.
17 **Horn, G.** and **Israelachvili, J. N.** Direct measurement of structural forces between two surfaces in a nonpolar liquid. *J. Chem. Phys.,* 1981, **75**(3), 1400–1411.
18 **Van Megen, W.** and **Snook, I.** Solvent structure and solvation forces between solid bodies. *J. Chem. Soc., Faraday Trans. II*, 1979, **75**, 1095–1102.
19 **Israelachvili, J. N., Mcguiggan, P. M.** and **Homola, A. M.** Dynamic properties of molecularly thin liquid films. *Science*, 1988, **240**, 189–191.
20 **Israelachvili, J. N.** Intermolecular and Surface Forces, 2nd edition, 1992 (Academic Press, London, Orlando, San Diego, New York, etc.).
21 **Homola, A. M., Israelachvili, J. N., Gee, M. L.** and **Mcguiggan, P. M.** Measurements of and relation between the adhesion and friction of two surfaces separated by molecularly thin liquid films. *Trans. ASME, J. Tribology*, 1989, **111**, 675–682.
22 **Lifshitz, E. M.** The theory of molecular attractive forces between solids. *Sov. Physics, JETP*, 1956, **2**, 73–83.